⌘ *Author's Choice*

THE JOURNAL OF BIOLOGICAL CHEMISTRY VOL. 286, NO. 13, pp. 11506–11518, April 1, 2011

Differential G-protein-coupled Receptor Phosphorylation Provides Evidence for a Signaling Bar Code*

Received for publication, June 19, 2010, and in revised form, November 30, 2010 Published, JBC Papers in Press, December 21, 2010, DOI 10.1074/jbc.M110.154526

Adrian J. Butcher[‡1], Rudi Prihandoko[‡1], Kok Choi Kong[‡], Phillip McWilliams[‡], Jennifer M. Edwards[§], Andrew Bottrill[¶], Sharad Mistry[¶], and Andrew B. Tobin[‡2]

From the [‡]Department of Cell Physiology and Pharmacology, [¶]Protein and Nucleic Acid Chemistry Laboratory, and [§]MRC Toxicology Unit, University of Leicester, Hodgkin Building, Lancaster Road, Leicester LE1 9HN, United Kingdom

G-protein-coupled receptors are hyper-phosphorylated in a process that controls receptor coupling to downstream signaling pathways. The pattern of receptor phosphorylation has been proposed to generate a "bar code" that can be varied in a tissue-specific manner to direct physiologically relevant receptor signaling. If such a mechanism existed, receptors would be expected to be phosphorylated in a cell/tissue-specific manner. Using tryptic phosphopeptide maps, mass spectrometry, and phospho-specific antibodies, it was determined here that the prototypical $G_{q/11}$-coupled M_3-muscarinic receptor was indeed differentially phosphorylated in various cell and tissue types supporting a role for differential receptor phosphorylation in directing tissue-specific signaling. Furthermore, the phosphorylation profile of the M_3-muscarinic receptor was also dependent on the stimulus. Full and partial agonists to the M_3-muscarinic receptor were observed to direct phosphorylation preferentially to specific sites. This hitherto unappreciated property of ligands raises the possibility that one mechanism underlying ligand bias/functional selectivity, a process where ligands direct receptors to preferred signaling pathways, may be centered on the capacity of ligands to promote receptor phosphorylation at specific sites.

Agonist occupation of G-protein-coupled receptors (GPCRs)[3] results in rapid receptor phosphorylation in a process that not only mediates the uncoupling of the receptor from its cognate G-protein but also drives G-protein-independent receptor signaling (1–3). It is now clear that GPCR phosphorylation is a complex regulatory mechanism involving an array of different protein kinases that include second messenger regulated kinases, members of the G-protein-coupled receptor kinase (GRK) family, as well as receptor tyrosine kinases and protein kinase CK2 and CK1α (2–4). The consequence of this kinase activity is the hyperphosphorylation of GPCRs at sites largely within the third intracellular loop and C-terminal tail, which in turn promotes the recruitment of arrestin proteins that mediate G-protein-independent signaling (1–4).

The complexity of GPCR phosphorylation allows for the possibility that receptors might be phosphorylated differentially in different cell types (5) and thereby provide a mechanism by which the same receptor subtype would have different signaling properties depending on the cell type in which the receptor is expressed (3). This notion has been supported by recent studies on the β_2-adrenergic receptor and CXC4R receptor where receptor phosphorylation by different members of the GRK family can mediate different signaling outcomes (6, 7). Furthermore, our own studies and the studies of others on the M_3-muscarinic receptor have demonstrated that phosphorylation of this receptor subtype by CK1α regulates receptor signaling to the phospholipase C and ERK pathways (8, 9), whereas phosphorylation mediated by protein kinase CK2 has no impact on ERK/phospholipase C but rather regulates the coupling of the receptor to the JNK pathway (5).

These studies suggest that one mechanism by which receptors might direct signaling to one pathway (*i.e.* JNK) in preference to another (*i.e.* ERK) might be via specific phosphorylation profiles of the receptor. By adopting a specific phosphorylation profile or "phosphorylation signature," a receptor could favor coupling to a particular pathway. In this way, the phosphorylation profile of a receptor could act as a "bar code" that encodes a particular signaling outcome (3, 10–12). Hence, in each tissue type a GPCR might adopt a different phosphorylation profile, or bar code, and this would contribute to tissue-specific signaling related to the physiological function of the receptor.

If such a regulatory mechanism existed, then it would be expected that receptors would be differentially phosphorylated in different cell types. We test this possibility in this study and present evidence that the M_3-muscarinic receptor is indeed differently phosphorylated in different cell and tissue types. Furthermore, we show that ligands can favor specific phosphorylation events that raise the possibility of ligand-specific phosphorylation and thereby a mechanism by which biased ligands could direct the preferential coupling of receptors to downstream signaling networks.

EXPERIMENTAL PROCEDURES

Materials—Unless otherwise stated, all biochemicals and reagents were from Sigma or from previously identified sources (5). Radioisotope [^{32}P]orthophosphate (specific activity 8500–9120 Ci/mmol), *myo*-[^{3}H]inositol (specific activity 25 Ci/mmol), and *N*-[^{3}H]methylscopolamine (specific activity

* This work was supported by Wellcome Trust Grant 047600 and Heptares Inc.
⌘ *Author's Choice*—Final version full access.
[1] Both authors contributed equally to this work.
[2] To whom correspondence should be addressed. Tel.: 116-2522935; Fax: 116-2231405; E-mail: tba@le.ac.uk.
[3] The abbreviations used are: GPCR, G-protein-coupled receptor; GRK, G-protein-coupled receptor kinase; CG, cerebellar granule.

83 Ci/mmol) were from PerkinElmer Life Sciences. The anti-muscarinic receptor antibodies used in this study were generated in-house against a glutathione *S*-transferase (GST) bacterial fusion protein containing the full third intracellular loop of the mouse M_3-muscarinic receptor (Arg^{252}–Thr^{491}). Where rabbit polyclonal antibodies were raised, the antibodies were first passed through a GST-affinity column to remove antibodies to GST and then purified by affinity chromatography on a column containing the receptor-fusion protein. In the case of mouse monoclonal antibodies, affinity purification against the antigen was carried out.

Phosphorylation-specific antibodies, anti-phosphoserine 384, 412, and 577, were raised against peptide sequences NSTKLPpSSDNLQ, HKLQAQKpSMDDRD, and YQQRQpSVIFHK, corresponding to amino acid residues 378–389, 405–418, and 572–583 of the mouse M_3-muscarinic receptor in which serines 384, 412, and 577 were phosphorylated. The 87-day programs, which included four immunizations, were performed by Eurogentec. The resulting antisera were purified against the immunizing peptides.

Generation of GST Fusion Constructs—Mouse M_3-muscarinic receptor third intracellular loop Arg^{252} to Thr^{491} and the C-terminal Lys^{548} to Leu^{589} were inserted into pGEX-2t to produce N-terminal GST fusions. *Escherichia coli* BL21 (DE3) IRL transformed with the fusion constructs or pGEX-2t alone was grown in LB medium containing 50 μg/ml ampicillin, 50 μg/ml chloramphenicol, and 1% w/v glucose; protein expression was induced by addition of isopropyl 1-thio-β-D-galactopyranoside to a final concentration of 200 μM.

Culture of CHO-M_3 Wild-type Stable Cell Lines—CHO cells stably expressing the wild-type M_3-muscarinic receptor were maintained in Ham's F-12 medium (Invitrogen) supplemented with 10% fetal calf serum (FCS), penicillin (50 units/ml), streptomycin (50 μg/ml), and geneticin G418 (500 μg/ml). Experiments were performed in Krebs/HEPES buffer (118 mM NaCl, 1.3 mM $CaCl_2$, 4.3 mM KCl, 1.17 $MgSO_4$, 4.17 mM $NaHCO_3$, 1.18 mM KH_2PO_4, 11.7 mM glucose, 10 mM HEPES (pH 7.4)) or in a modified Krebs/HEPES buffer as indicated.

Preparation and Primary Culture of Mouse Cerebellar Granule Neurons—Mouse CG neurons were prepared and cultured as described previously (5), trypsin- dissociated, and plated on poly-D-lysine-coated 6-well plates at a density of 2×10^6 cells well. The neurons were maintained in Eagle's basal medium (Invitrogen) supplemented with 20 mM KCl, penicillin/streptomycin, and 10% FCS. After 48 h, cytosine arabinoside (10 μM) was added to prevent glial cell proliferation, and the culture was continued for 7–8 days. Experiments were then performed on cells that were washed and then maintained in CSS-25 buffer (120 mM NaCl, 1.8 mM $CaCl_2$, 25 mM KCl, 15 mM glucose, 25 mM HEPES (pH 7.4)).

M_3-muscarinic Receptor Purification and Mass Spectrometry—For the mass spectrometry experiments, a stably transfected CHO cell line was generated that expressed a mouse M_3-muscarinic receptor HA-tagged at the C terminus. For receptor purification, 20 confluent T175 flasks were harvested and resuspended in 40 ml of Krebs/HEPES buffer and stimulated with methacholine (100 μM, 5 min). Membranes were then prepared and solubilized by addition of 5 ml of PBS containing 1% Nonidet P-40 plus a mixture of protease and phosphatase inhibitors. After centrifugation at 20,000 $\times$ *g*, the resulting supernatant was diluted 1:1 with PBS, and the receptor was then purified on anti-HA affinity resin (Roche Diagnostics). After extensive washing with solubilization buffer containing 0.5% Nonidet P-40, the resin was resuspended in 2$\times$ SDS-PAGE sample buffer. The sample was resolved by SDS-PAGE on 8% gels and stained with colloidal Coomassie Blue. Purified M_3-muscarinic receptors were excised from the polyacrylamide and washed three times for 15 min with 100 mM ammonium bicarbonate. Reduction and alkylation of cysteines were performed by addition of 10 mM dithiothreitol (DTT) in 50 mM ammonium bicarbonate at 60 °C for 30 min followed by addition 100 mM iodoacetamide in 50 mM ammonium bicarbonate for 30 min in the dark. Gel slices were washed three times for 5 min with 50 mM ammonium bicarbonate containing 50% acetonitrile and incubated overnight at 37 °C in 50 mM ammonium bicarbonate containing 1 μg of sequencing grade trypsin (Promega).

LC-MS/MS was carried out on each sample using a 4000 Q-Trap mass spectrometer (Applied Biosystems, Warrington, UK). Peptides resulting from in-gel digestion were loaded at a high flow rate onto a reverse-phase trapping column (0.3 mm inner diameter $\times$ 1 mm), containing 5 μm of C18 300 Å Acclaim PepMap media (Dionex, UK) and eluted through a reverse-phase capillary column (75 μm inner diameter $\times$ 150 mm) containing Symmetry C18 100 Å media (Waters) that was self-packed using a high pressure packing device (Proxeon Biosystems, Odense, Denmark). The output from the column was sprayed directly into the nanospray ion source of the 4000 Q-Trap mass spectrometer. Additional mass spectrometry experiments were performed on an LTQ Orbitrap mass spectrometer by "FingerPrints" Proteomics Facility (College of Life Sciences, University of Dundee).

The resulting spectra were searched against the UniProtKB/SwissProt data base using MASCOT software (Matrix Science Ltd.) with peptide tolerance set to 5 ppm for LTQ OrbiTrap data or 0.1 Da for 4000 Q-Trap data, and the MS/MS tolerance was set to 0.6 Da. Fixed modifications were set as carbamidomethyl cysteine with variable modifications of phosphoserine, phosphothreonine, phosphotyrosine, and oxidized methionine. The enzyme was set to trypsin/P, and up to two missed cleavages were allowed. Peptides with a Mascot score greater than 20 and where the probability (*p*) that the observed match was a random event was <0.05 were included in the analysis. The spectra of peptides reported as being phosphorylated were interrogated manually to confirm the precise sites of phosphorylation.

[^{32}P]Orthophosphate Labeling and M_3-muscarinic Receptor Immunoprecipitation—In vivo [^{32}P]orthophosphate labeling, receptor solubilization, and immunoprecipitation were conducted as described previously (5). In brief, CHO cells stably expressing the human M_3-muscarinic receptor were grown in 6-well plates, washed, and incubated for 1 h in KH_2PO_4-free Krebs buffer containing 100 μCi/ml [^{32}P]orthophosphate (PerkinElmer Life Sciences). Cells were then stimulated with 0.1 mM methacholine for 5 min and lysed in RIPA buffer (2

mM EDTA, 20 mM β-glycerophosphate, 160 mM NaCl, 1% Nonidet P-40, 0.5% deoxycholate, 10 mM Tris (pH 7.4)). M_3-muscarinic receptors were immunoprecipitated using an in-house anti-M_3-muscarinic receptor polyclonal antibody (5). Immunoprecipitated proteins were resolved by SDS-PAGE on 8% gels, transferred to nitrocellulose membrane, and visualized by autoradiography. The membrane was subsequently blocked and immunoblotted with another in-house anti-mouse M_3-muscarinic receptor monoclonal antibody for the detection of total receptors. To dephosphorylate the immunoprecipitated receptor, the immune complexes were washed three times with 10 mM Tris (pH 7.4) containing 0.25% *n*-octyl glucoside before treatment with calf intestinal phosphatase (20 units per reaction) for 2 h at 37 °C. Receptors were then resolved by SDS-PAGE on 8% gels and immunoblotted with phosphorylation-specific antibodies.

For phosphopeptide mapping, CHO-M3 cells were labeled with 100 μCi/ml of [^{32}P]orthophosphate. Stimulation and immunoprecipitation were carried out as described above. The immunoprecipitated samples of one entire 6-well plate of CHO cells were pooled and resolved by SDS-PAGE on 8% gels. Tryptic phosphopeptide maps were prepared as described previously (5). The resolved phosphopeptides were then visualized using a STORM 820 phosphorimager (GE Healthcare) and quantified using AlphaEaseFC software (Alpha Innotech).

M_3-muscarinic Receptor Immunoprecipitation from Tissue Samples—To establish the phosphorylation status of M_3-muscarinic receptors in preparations from the hippocampus, cerebral cortex, and whole pancreas, tissues from adult wild-type or adult M_3-muscarinic receptor knock-out mice on a mixed genetic background (129/SvEv × CF1) (25) were extracted into ice-cold HIB buffer (25 mM HEPES (pH 7.4), 120 mM NaCl, 5 mM KCl, 9.1 mM glucose) containing protease inhibitors and phosphatase inhibitors (Complete EDTA-free, PhosStop, Roche Diagnostics). Membranes were prepared and solubilized in buffer composed of 20 mM Tris (pH 7.4), 150 mM NaCl, 3 mM EDTA, and 1% Nonidet P-40. The receptor was immunoprecipitated with the anti-M_3-muscarinic receptor monoclonal antibody. Immune complexes were washed three times in solubilization buffer and resuspended in 2× SDS-PAGE sample buffer. Receptors were separated by SDS-PAGE on 8% gels, transferred on to nitrocellulose membranes, and immunoblotted with anti-phosphoserine 384, anti-phosphoserine 412, or anti-phosphoserine 577 antibodies. For the detection of total receptors, membranes were stripped and re-probed with an anti-mouse M_3 muscarinic receptor antibody. Western blots were digitized and quantified as described above.

Total [^{3}H]Inositol Phosphate Accumulation Assay—To assess agonist efficacy, total [^{3}H]inositol phosphate accumulation assay was carried out CHO-m3 cells. In brief, cells seeded at 100,000 cells/well in 24-well plates were labeled with 2.5 μCi/ml *myo*-[^{3}H]inositol (PerkinElmer Life Sciences) for 24 h at 37 °C. Cells were washed twice in Krebs/HEPES buffer (pH 7.4) and incubated with 10 mM LiCl for 20 min at 37 °C. Appropriate concentrations of agonist were added for 10 min to stimulate [^{3}H]inositol phosphate production. Reactions were terminated by rapid aspiration of the buffer and addition of 1 M ice-cold trichloroacetic acid (500 μl). Cell lysates were transferred to centrifuge tubes and incubated with 10 mM EDTA (50 μl) and 1,1,2-trichlorofluoroethane/tri-*n*-octylamine (1:1, v/v, 500 μl) for 15 min at room temperature. Samples were centrifuged at 20,000 × *g* for 4 min. An ~400-μl aliquot from the top layer was recovered and transferred to fresh tubes containing 60 mM $NaHCO_3$. [^{3}H]Inositol mono-, bis-, and trisphosphate ([^{3}H]InsP*x*) fraction was recovered by anion exchange chromatography as follows: Dowex-1 (formate form) columns were regenerated with 10 ml of ammonium formate (2 M), formic acid (0.1 M) and washed thoroughly with distilled water. Samples were applied to the columns, and the columns washed with 10 ml of distilled water. Columns were then washed with ammonium formate (60 mM), sodium tetraborate (10 mM) solution. Total [^{3}H]InsP*x* was eluted in 10 ml of ammonium formate (0.75 M), formic acid (0.1 M) and collected in large scintillation vials. A 5-ml aliquot from the eluate was mixed with 10 ml of SafeFluor scintillation mixture, and radioactivity was detected by liquid scintillation counting.

Muscarinic Receptor Expression Levels—The expression levels of the M_3-muscarinic receptor were determined in membranes isolated from the hippocampus, cortex, and submandibular salivary gland by subtracting the specific binding of the muscarinic antagonist *N*-[^{3}H]methylscopolamine obtained from wild-type mice from that obtained from M_3-muscarinic receptor knock-out mice. *N*-[^{3}H]Methylscopolamine binding was conducted as described previously (13). The M_3-muscarinic receptor expression levels in hippocampus, cortex, and submandibular gland were 258, 351, and 335 fmol/mg protein, respectively.

Immunocytochemistry of Salivary Submandibular Glands—The submandibular glands from wild-type mice or M_3-muscarinic receptor gene knock-out mice were dissected and fixed in 10% neutral buffered formalin. The fixed tissue were embedded in paraffin and processed on a Shandon Citadel 2000 where serial sections (5 μm) were cut. Sections where dewaxed in xylene, dehydrated through alcohol, and then washed with distilled water. The sections were then treated for microwave antigen retrieval in a Sanyo Shower Wave 1000-watt microwave, at 700 watts for 20 min in a 0.01 M citrate buffer (pH 6.0). Sections were then permeabilized with Triton X-100, and the M_3-muscarinic receptor was stained with either anti-M_3 muscarinic receptor antibodies or receptor phospho-specific antibodies used at a dilution of 1:200 using methods described previously (5, 14).

Data Analysis—Data presented are means ± S.E. of at least three determinations, and statistically significance differences were determined using analysis of variance followed by the Bonferroni post test. Significance was accepted at $p < 0.05$.

RESULTS

Phosphorylation Profile of the M_3-muscarinic Receptor in Three Cell Types—The phosphorylation profile of the mouse M_3-muscarinic receptor expressed in Chinese hamster ovary (CHO) cells as a recombinant protein or as an endogenously expressed protein in the mouse insulinoma

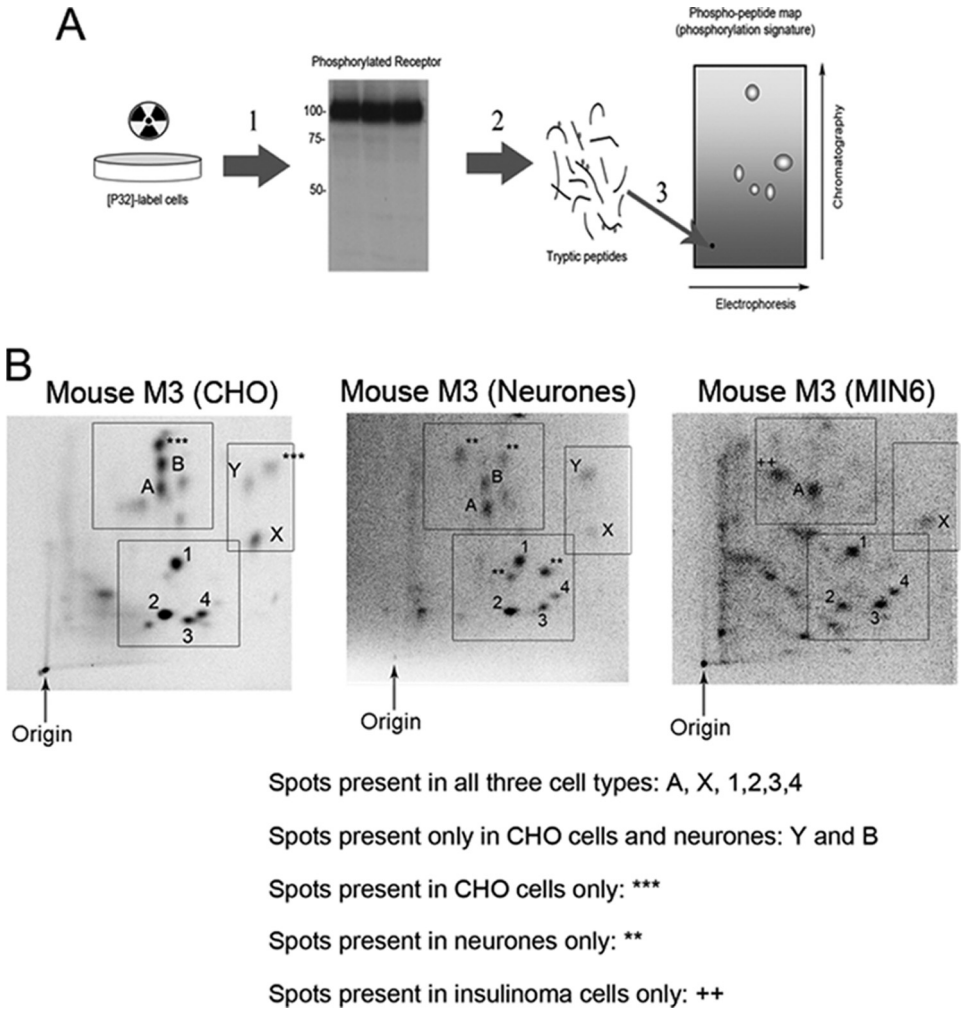

FIGURE 1. **Differential phosphorylation of the M_3-muscarinic receptor in CHO cells, MIN6 insulinoma cells, and CG neurons.** *A,* schematic of the method employed in generating a tryptic phosphopeptide map. *Step 1,* cells are labeled with [^{32}P]orthophosphate and stimulated with agonist for 5 min. The cells are then lysed and the receptors immunoprecipitated and resolved by SDS-PAGE. An autoradiograph of the gel determines the position of the radiolabeled receptor, which is excised from the gel. *Step 2,* excised gel band is tryptically digested. *Step 3,* tryptic digest is spotted onto a cellulose plate and subjected to electrophoresis and ascending chromatography to resolve the tryptic peptides. The position of the phosphopeptides is determined by exposing the gel in a phosphorimager. *B,* tryptic phosphopeptide maps of the mouse M_3-muscarinic receptor immunoprecipitated from CHO-m3 (*CHO*), CG neurons, and MIN6 insulinoma cells. For ease of viewing, the autoradiographs are divided into three sections denoted by the *boxes*. Phosphopeptide "spots" are labeled to designate spots that are unique to a cell type or shared between cell types (see key on the figure). Each autoradiograph is representative of at least three independent experiments.

cell line, MIN6, and mouse primary CG neurons was investigated. The receptor was immunoprecipitated from [^{32}P]orthophosphate-labeled cells and digested with trypsin. The tryptic phosphopeptides were then resolved by two-dimensional chromatography, and an autoradiograph was obtained to provide a phosphopeptide map (Fig. 1*A*).

The phosphopeptide map from the three cell types revealed a quartet of phosphopeptides labeled 1–4 that served to orient the map (Fig. 1*B*). These peptides were seen in all three cell types as were phosphopeptides labeled *A* and *X* (Fig. 1*B*). In contrast, there were a number of phosphopeptides that were observed in only one of the three cell types. Thus, phosphopeptides labeled with three asterisks were only observed in receptors derived from CHO cells (Fig. 1*B*). Four phosphopeptides labeled with two asterisks were only observed in CG neurons, and the phosphopeptide labeled with two plus signs was only observed in insulinoma cells. There were some phosphopeptides that were shared just between two cell types as illustrated by phosphopeptides Y and B that are shared between CHO cells and CG neurons.

These studies demonstrated that although there were common features in the phosphorylation profiles of the M_3-muscarinic receptor in the three cell types investigated, there were also specific differences that make the overall phosphorylation profile of the M_3-muscarinic receptor expressed in each of the cell types unique.

Mass Spectrometry Identification of Phospho-acceptor Sites and Generation of Phospho-specific Antibodies—Although the phosphopeptide maps described above illustrate differential receptor phosphorylation, these studies do not reveal the precise sites of phosphorylation. To do this, we conducted a mass spectrometric analysis of the phospho-acceptor sites on the M_3-muscarinic receptor expressed in CHO cells. These studies revealed 13 serine and 2 threonine phospho-acceptor sites in the third intracellular loop and one serine (Ser^{577}) in the C-terminal tail (Fig. 2).

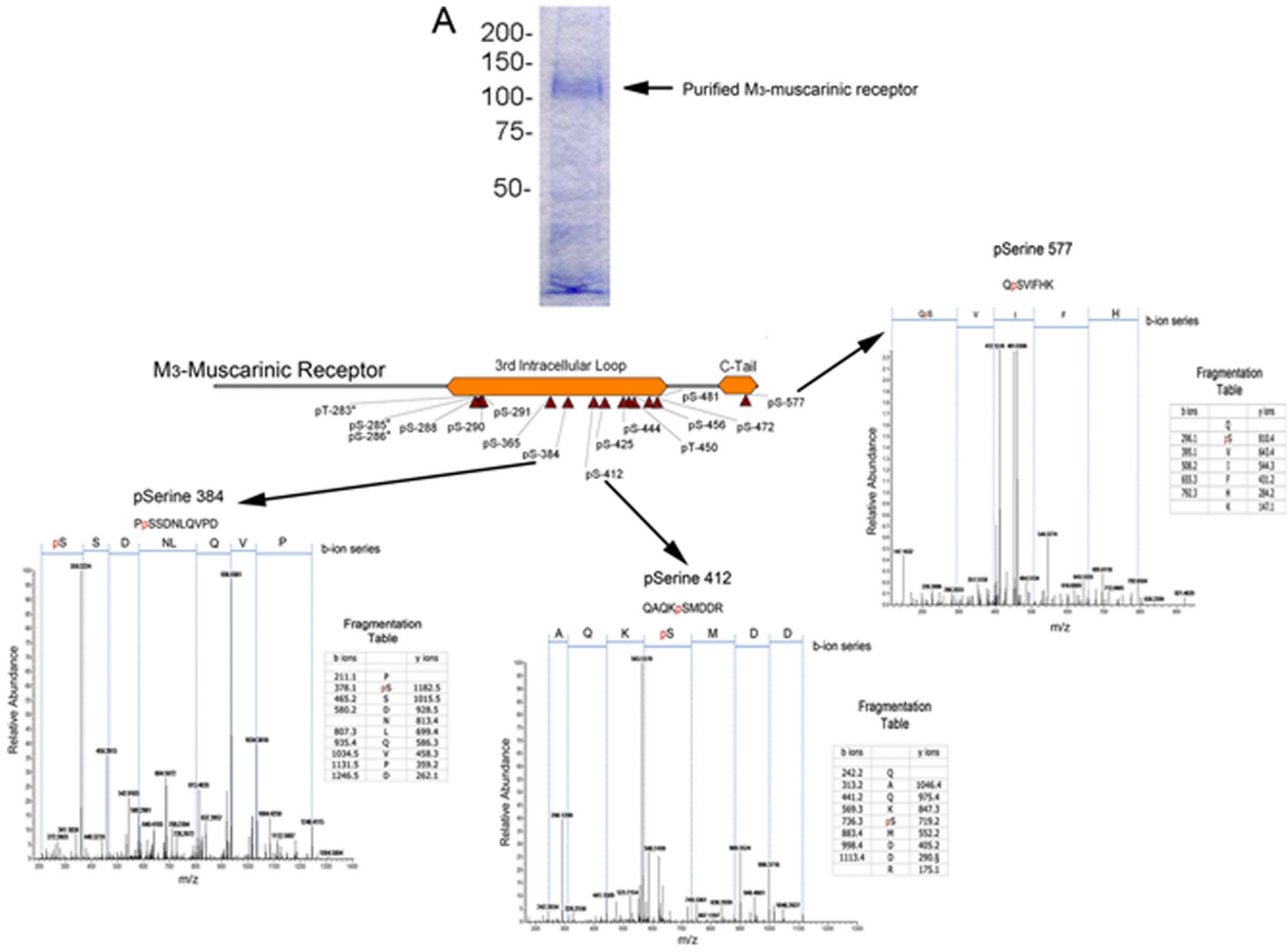

B M3-muscarinic receptor phospho-peptides

Peptide Sequence	Mascot Ion score	Delta PPM	Residue number
(K)RM**S**LIK(E)	23.99	0.5373	479-484
(K)TR**S**QITK(R)	36.25	-0.8052	470-476
(R)Q**S**VIFHK(R)	20.89	-0.7794	576-582
(R)KRM**S**LIK(E)	27.96	-1.205	478-484
(R)AIY**S**IVLK(L)	34.39	1.252	362-369
(K)TTAALPL**S**FK(E)	60.95	-1.022	449-458
(R)KRM**S**LIKEK(K)	24.65	-0.7566	478-486
(K)LQAQK**S**MDDR(D)	46.22	0.04623	407-416
(K)LP**S**SDNLQVPDK(D)	49.22	0.6567	382-393
(R)Sc**S**YELQQQGTK(R)	79.62	0.9672	288-300
(R)Sc**S**YELQQQGTK(R)	66.81	0.9747	288-300
(R)**S**c**S**YELQQQGTK(R)	60.23	0.9759	288-300
(R)**S**c**S**YELQQQGTK(R)	48.1	1.768	288-300
(R)Sc**SS**YELQQQGTK(R)	57.32	1.768	288-300
(R)KQQYQQRQ**S**VIFHK(R)	24.06	32.7	569-582
(K)LQAQK**S**MDDRDNcQK(D)	40.75	-0.3186	407-421
(V)DKT**T**AALPLSFKEATLAKR(F)	78.51	-5.338	447-465
(K)TSDTNS**S**VDKTTAALPLSFK(E)	42.2	1.089	439-458
(K)TSDTN**S**SVDKTTAALPLSFK(E)	38.06	1.089	439-458
(R)NAHKLQAQK**S**MDDRDNcQK(D)	22.53	-0.01933	403-421
(K)LP**S**SDNLQVPDKDLGTMDVER(N)	80.59	-56.18	382-402
(K)ELAGLQASGTEAEAENFVHPTG**S**SR(S)	49.18	393	263-287
(K)ELAGLQASGTEAEAENFVHP**T***G**S***S***R(S)	41.8	1.326	263-287
(R)TKELAGLQASGTEAEAENFVHPTG**S**SR(S)	34.08	-0.7901	261-287
(S)MDDRDNcQKDF**S**KLPIQLESAVDTAK(T)	65.79	-140.5	413-438

C Summary of M3-muscarinic receptor phosphorylation

```
1   MTLHSNSTTS PLFPNISSSW VHSPSEAGLP LGTVSQLDSY NISQTSGNFS
51  SNDTSSDPLG GHTIWQVVFI AFLTGFLALV TIIGNILVIV AFKVNKQLKT
101 VNNYFLLSLA CADLIIGVIS MNLFTTYIIM NRWALGNLAC DLWLSIDYVA
151 SNASVMNLLV ISFDRYFSIT RPLTYRAKRT TKRAGVMIGL AWVISFVLWA
201 PAILFWQYFV GKRTVPPGEC FIQFLSEPTI TFGTAIAAFY MPVTIMTILY
251 WRIYKETEKR TKELAGLQAS GTEAEAENFV HPTGSSRSCS SYELQQQGTK
301 RSSRRKYGGC HFWFTTKSWK PSAEQMDQDH SSSDSWNNND AAASLENSAS
351 SDEEDIGSET RAIYSIVLKL PGHSTILNST KLPSSDNLQV PDKDLGTMDV
401 ERNAHKLQAQ KSMDDRDNCQ KDFSKLPIQL ESAVDTAKTS DTNSSVDKTT
451 AALPLSFKEA TLAKRFALKT RSQITKRKRM SLIKEKKAAQ TLSAILLAFI
501 ITWTPYNIMV LVNTFCDSCI PKTYWNLGYW LCYINSTVNP VCYALCNKTF
551 RTTFKMLLLC QCDKRKRRKQ QYQQRQSVIF HKRVPEQAL
```

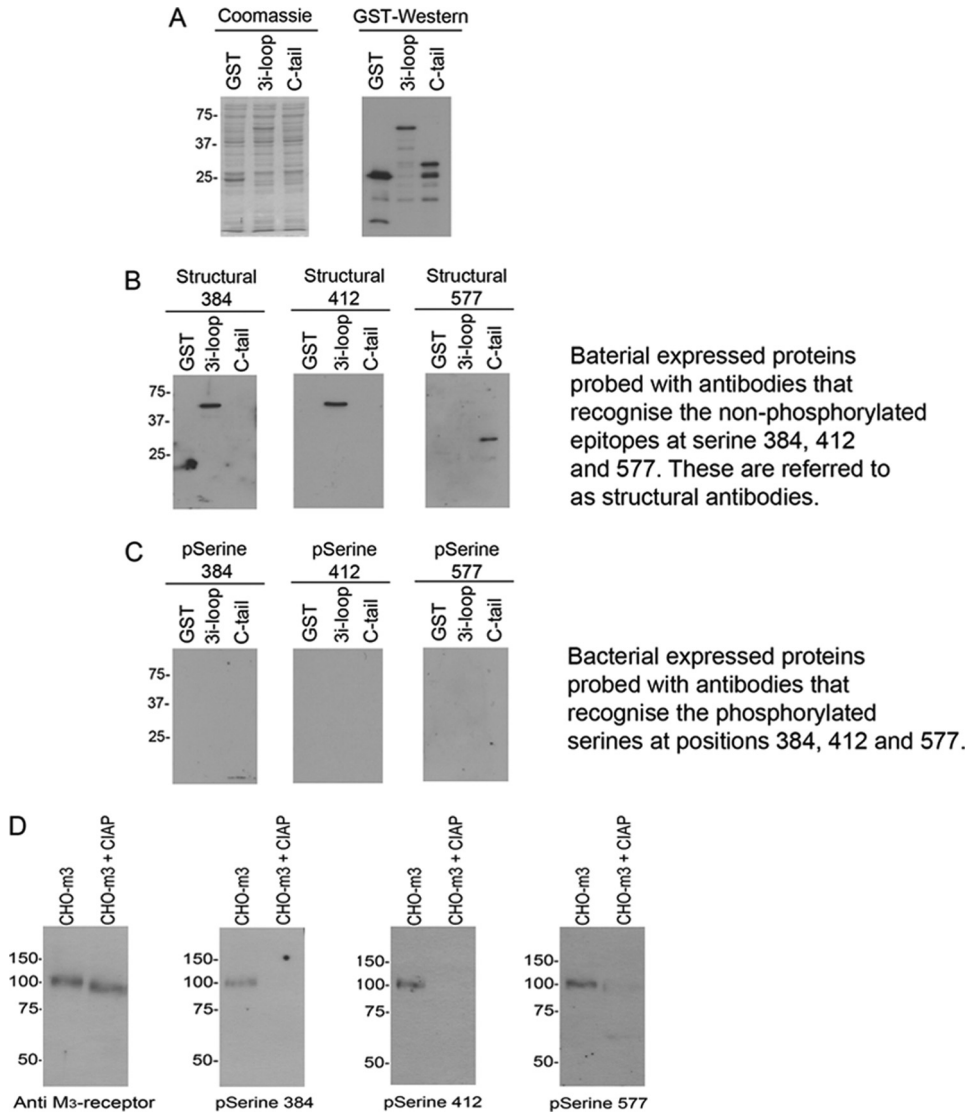

FIGURE 3. **Characterization of phospho-specific antibodies raised against serines 384, 412, and 577.** Crude bacterial lysates containing either GST or GST fused to the third intracellular loop of the mouse M_3-muscarinic receptor (*3i-loop*) or C-terminal tail (*C-tail*) were probed with the following antibodies. *A,* antibodies against GST. This served as a loading control as did the Coomassie stain of gel. *B,* nonphospho-specific antibodies (structural) generated from the immunization. *C,* purified phospho-specific antibodies. *D,* CHO cells expressing the recombinant mouse M_3-muscarinic receptor were stimulated with methacholine (100 μM) for 5 min. The receptor was then solubilized and immunoprecipitated with an M_3-muscarinic receptor specific monoclonal antibody. The nitrocellulose was then probed with the phospho-specific antibodies to serines 384, 412, and 577. Where indicated the immunoprecipitated receptor was treated with calf intestinal phosphatase (*CIAP*) to remove phosphates from the receptor. The sample was also probed with an antibody against the M_3-muscarinic receptor (*anti-M_3-receptor*) as a loading control. The data shown are representative of at least two experiments.

Phospho-specific antibodies were raised to phosphorylated Ser^{384} and Ser^{412} in the third intracellular loop and Ser^{577} in the C-terminal tail. These were chosen because they represented phosphorylated residues that were not within a cluster of phosphorylation sites (which would have made specific antibody generation difficult) and that were sites determined to have high antigenicity. The antiserum from each of the immunizations was subjected to affinity purification that separated nonphospho-specific antibodies (structural antibodies) and phospho-specific antibodies. To test the specificity of the purified antiserum, the nonphosphorylated epitopes present in bacterial glutathione *S*-transferase (GST) fusion proteins containing either the third intracellular loop of the receptor or the C-terminal tail were probed in Western blots with the structural antibody and the phospho-specific receptor antibodies (Fig. 3, *A*–*C*). In these experiment, the structural anti-

FIGURE 2. **Determination of the sites of phosphorylation on the M_3-muscarinic receptor by mass spectrometry.** *A,* recombinant mouse M_3-muscarinic receptor expressed in CHO cells was stimulated with methacholine (100 μM) for 5 min. Membranes were then prepared, and the receptor was purified. The receptor was subjected to tryptic digestion, and the peptides were analyzed by mass spectrometry. Shown is a schematic indicating the phospho-acceptor sites in the third intracellular loop and C-terminal tail. Also shown are typical LC-MS/MS traces that identify serines 384, 412, and 577 as phosphoserines. *B,* list of the phosphopeptides identified by LC-MS/MS. The phosphorylated residue is highlighted in *red*. Note that where residues are labeled with an *asterisk,* it was not possible to determine which of the residues were phosphorylated. All the peptides shown were observed in at least two independent experiments. *C,* schematic of the full amino acid sequence of the mouse M_3-muscarinic receptor indicating the position of the phosphorylated residues in *red* and *underlined*.

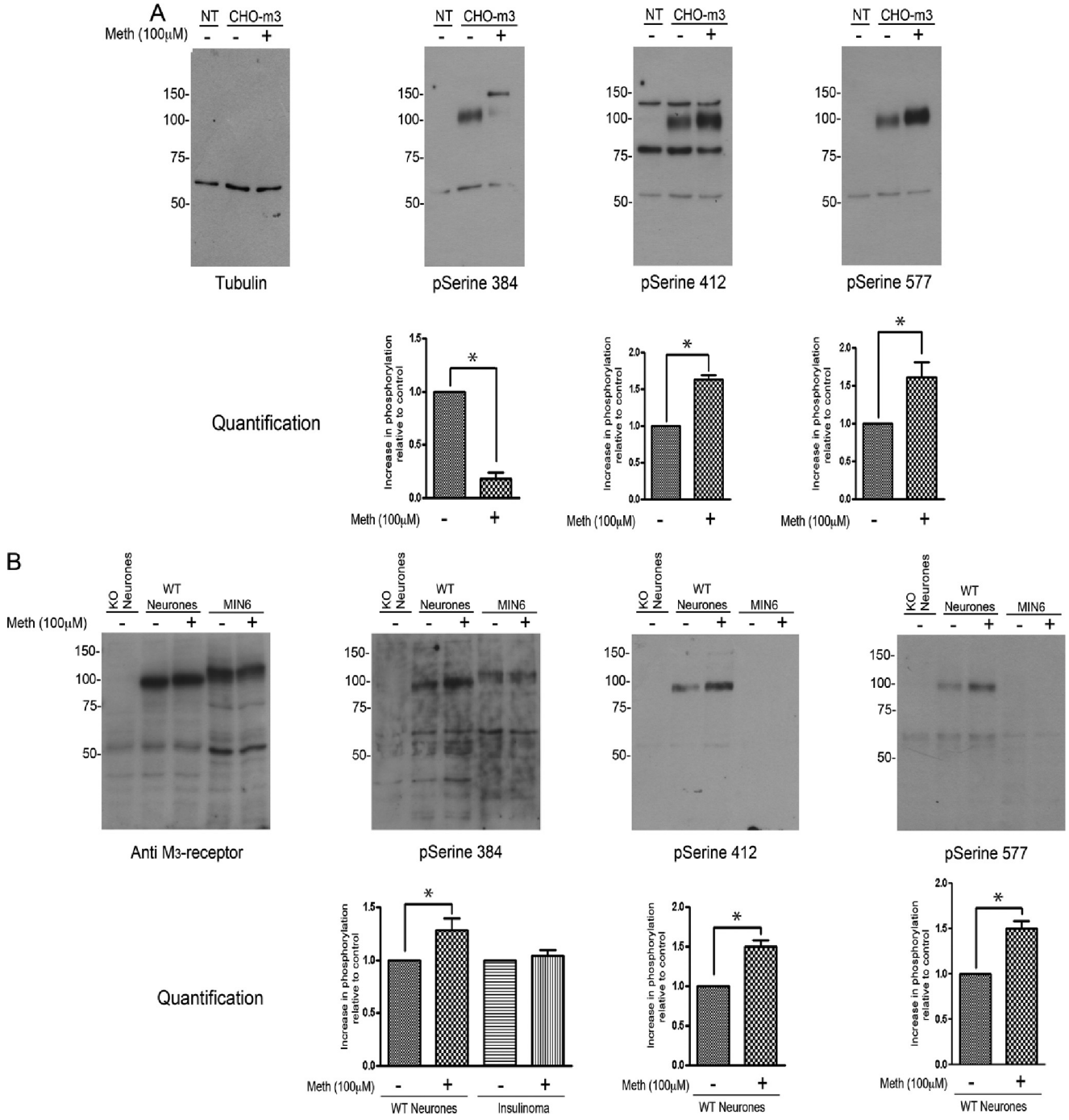

FIGURE 4. **Phospho-specific antibodies reveal differential phosphorylation of the M_3-muscarinic receptor.** *A,* either nontransfected CHO cells (*NT*) or CHO cells expressing the mouse M_3-muscarinic receptor (*CHO-m3*) were stimulated with or without methacholine (*Meth*) for 5 min. The cells were then lysed, and the lysate was probed in a Western blot with receptor phospho-specific antibodies. Shown also is a loading control probed for tubulin. *Graphs* representing quantification of the blots are shown *below* the autoradiographs. *B,* MIN6 insulinoma cells and primary cultures of CG neurons derived from wild-type mice (*WT*) or mice where the M_3-muscarinic receptor was knocked out (*KO*) were processed as described in *A* above. As a loading control, the lysate was probed for total M_3-muscarinic receptor content (*anti-M_3-receptor*). Shown are representative blots and *below* each blot graphical quantification. Graphs present the means ± S.E. of three independent experiments. *, $p < 0.05$ (*t* test).

bodies reacted with the appropriate fusion protein. The phospho-specific antibody fraction did not recognize the GST fusion proteins (Fig. 3, *B* and *C*). The phospho-specific antibodies did, however, identify the intact M_3-muscarinic receptor immunoprecipitated from transfected CHO cells (Fig. 3*D*). This immunoreactivity was lost following de-phosphorylation with calf intestinal phosphatase (Fig. 3*D*).

Determination of Cell Type-specific M_3-muscarinic Receptor Phosphorylation Using Receptor Phospho-specific Antibodies—The phosphorylation status of the M_3-muscarinic receptor at residues 384, 412, and 577 was investigated on receptors expressed in CHO cells, CG neurons, and MIN6 insulinoma cells (Fig. 4). Receptors derived from CHO cells showed high basal levels of phosphorylation on Ser^{384} that fell by 82% fol-

lowing receptor stimulation with the full agonist methacholine. In contrast, agonist stimulation increased phosphorylation on Ser^{384} by 28% in receptors expressed in CG neurons (Fig. 4*A*). In MIN6 cells, the receptor was basally phosphorylated on Ser^{384} and was not changed following agonist stimulation (Fig. 4*B*). These data demonstrate that phosphorylation at Ser^{384} was regulated differentially in the three cell types.

Analysis of the phosphorylation status of the receptor at Ser^{577} also showed the importance of cell background. In CHO cells and CG neurons, Ser^{577} phosphorylation was increased following agonist stimulation by 61 and 50%, respectively (Fig. 4, *A* and *B*). Interestingly there was no evidence of basal or agonist-mediated phosphorylation at Ser^{577} from receptors expressed in MIN6 cells (Fig. 4*B*).

Similarly, there was clear agonist-mediated phosphorylation at Ser^{412} from receptors derived from CHO cells and CG neurons. However, there was no evidence for Ser^{412} phosphorylation on receptors expressed in MIN6 cells (Fig. 4, *A* and *B*).

Analysis of in Vivo M_3-muscarinic Receptor Phosphorylation—To evaluate differential phosphorylation of the M_3-muscarinic receptor *in vivo*, membranes were prepared from the hippocampus, cerebral cortex, and pancreas from either wild-type mice or from mice where the M_3-muscarinic receptor gene had been knocked out. The membranes were then solubilized; the M_3-muscarinic receptor was immunoprecipitated with a receptor-specific monoclonal antibody, and the immunoprecipitate was probed in Western blots with receptor phospho-specific antibodies. In these experiments, the M_3-muscarinic receptor expressed in the hippocampus was determined to be phosphorylated equally on Ser^{318} and Ser^{412} but was phosphorylated to a lesser extent on $serine^{577}$ (Fig. 5*A*). The phosphorylation profile for the receptor appeared different in the cerebral cortex where the receptor was equally phosphorylated on Ser^{318} and Ser^{577} but less phosphorylated on Ser^{412} (Fig. 5*A*). The receptor showed a further unique phosphorylation profile in the pancreas where the receptor was generally poorly phosphorylated, showing a weak signal for phosphorylation on Ser^{318} and Ser^{412} but no detectable phosphorylation of Ser^{577} (Fig. 5*A*).

The molecular weight of the M_3-muscarinic receptor immunoprecipitated from the pancreas (Fig. 5*A*) and from MIN6 insulinoma cells (Fig. 4*B*) was observed to be greater than that in the brain and CHO cells. The reason for this is likely to be differential glycosylation because the receptor was poorly phosphorylated in pancreatic cell/tissue types; hence, phosphorylation was not likely to be a major contributory factor in the apparently high molecular weight of the receptor in these experiments.

We also investigated the phosphorylation status of the M_3-muscarinic receptor in salivary submandibular glands. However, we were not able to detect the receptor in Western blots from this tissue probably because the receptor was subjected to proteolysis. We were, however, able to detect the receptor by immunocytochemistry where the M_3-muscarinic receptor was determined to be expressed in the excretory cells as well as in the cells of the excretory ducts (Fig. 5*B*). In these experiments weak staining for the receptor phosphorylated on Ser^{384} and Ser^{412} was detected, although there was stronger staining for phosphorylation on Ser^{577} (Fig. 5*B*).

Hence, the phosphorylation profile of the M_3-muscarinic receptor was different in each of the four tissues. This difference is illustrated as a bar code in Fig. 5*C*.

Differential Regulation of Phosphorylation by Different Muscarinic Receptor Agonists—The studies above provide evidence that the phosphorylation status of the M_3-muscarinic receptor is dependent on the cell and tissue type in which the receptor is expressed. We extended this analysis by investigating if different agonists working at the receptor expressed in the same cell type could mediate different receptor phosphorylation profiles. To this end, the phosphorylation profile of the human M_3-muscarinic receptor expressed in CHO-m3 cells following stimulation by the agonists methacholine, pilocarpine, and arecoline was investigated. Previous studies had established that methacholine acts as a full agonist at muscarinic receptors and pilocarpine and arecoline as partial agonists (15, 16).

In this study, assays of inositol phosphate accumulation (InsP*x*) established methacholine as a full agonist at the M_3-muscarinic receptor and arecoline and pilocarpine as partial agonists (Fig. 6*A*). Consistent with previous studies (15, 16), the rank order of potency and maximal response (efficacy) for the InsP*x* response was methacholine > arecoline > pilocarpine (Fig. 6*A*). In phosphorylation assays, all three agonists stimulated an increase in total receptor phosphorylation with the same rank order of efficacy as that observed in the InsP*x* assay (Fig. 6*B*).

To determine the rank order of efficacy of the agonists at individual phosphorylation sites, phosphopeptide maps were generated following stimulation with the three agonists (Fig. 7, *A–E*). In these experiments, the relative intensity of four spots (*labeled 1–4*, Fig. 7) on the phosphopeptide map were compared. Spots 1 and 3 were significantly increased over basal when cells when stimulated with methacholine (Fig. 7, *B* and *D*). No significant changes in the phosphorylation of spot 1 or 3 were observed following stimulation with either arecoline or pilocarpine (Fig. 7*B*). Interestingly, spot 2 was highly phosphorylated in the basal state but became de-phosphorylated following methacholine stimulation (Fig. 7*C*). De-phosphorylation of spot 2 was also observed, but to a lesser extent, following stimulation with arecoline (Fig. 7*C*). No significant de-phosphorylation was observed in spot 2 with pilocarpine (Fig. 7*C*). Hence, the changes in phosphorylation observed for spots 1–3 more or less followed the expected rank order of efficacy for the three agonists. This, however, was in contrast to the phosphorylation of spot 4. Here, all three agonists increased phosphorylation at spot 4 with equivalent efficacy (Fig. 7*E*).

To further investigate this phenomenon, phospho-specific antibodies to Ser^{384}, Ser^{412}, and Ser^{577} were used to probe the effects of the three agonists on specific phosphorylation events on the M_3-muscarinic receptor in CHO-m3 cells. The receptor showed high basal levels of Ser^{384} phosphorylation, which were significantly decreased by methacholine treatment (Fig. 8*A*). Here, arecoline and pilocarpine also decreased phosphorylation at Ser^{384} with the following rank order of

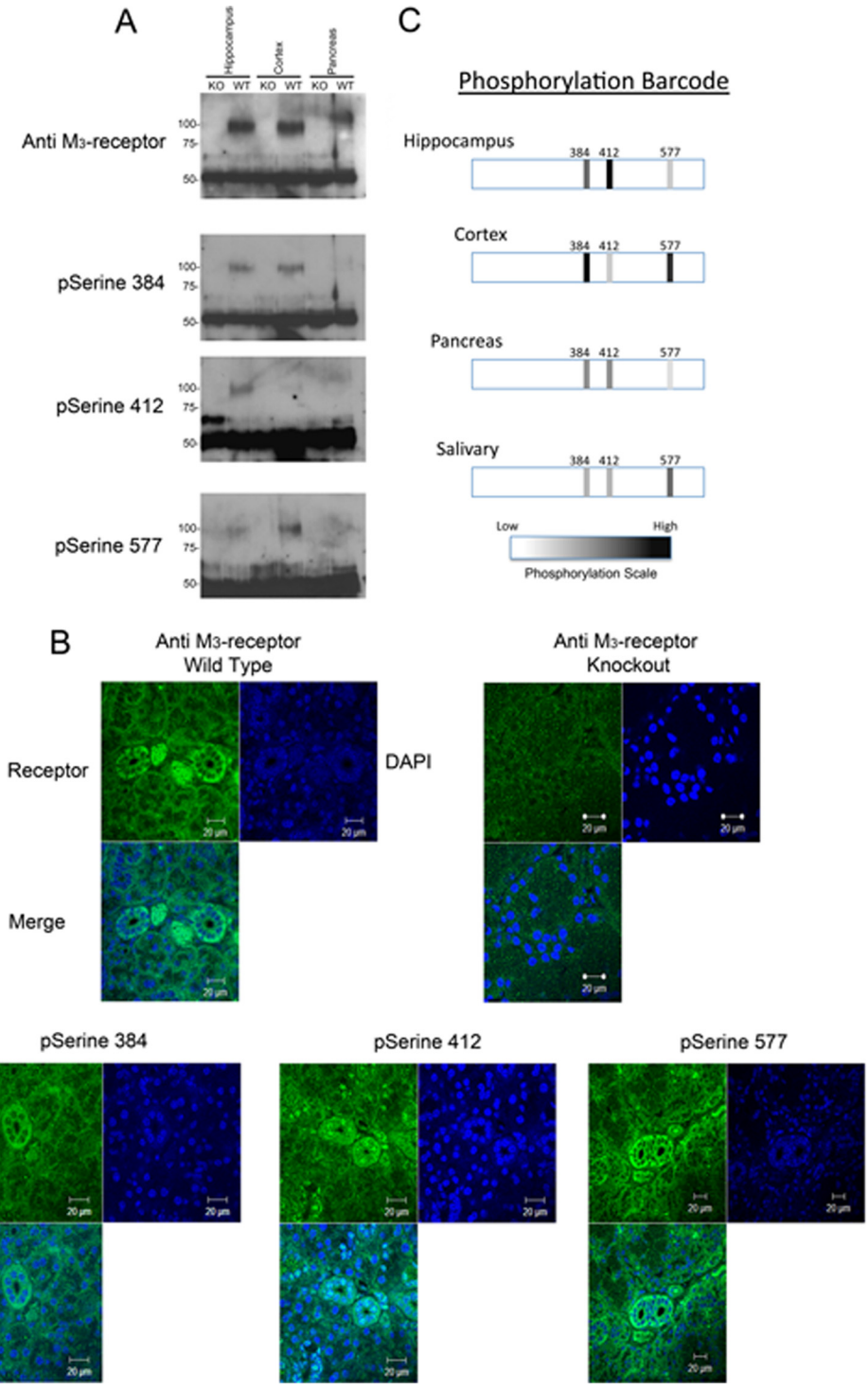

FIGURE 5. **Differential phosphorylation of the M_3-muscarinic receptor in the central nervous system, pancreas, and salivary glands.** *A,* membranes from cerebral cortex, hippocampus, and pancreas were prepared from wild-type (*WT*) and M_3-muscarinic receptor gene knocked out (*KO*) mice. Membranes were solubilized, and the M_3-muscarinic receptor was immunoprecipitated using a receptor monoclonal antibody. The immunoprecipitate was probed in Western blots with M_3-muscarinic receptor phospho-specific antibodies against phosphoserine 384, 412, and 577. Shown also is a loading control probed for total M_3-muscarinic receptor (*anti-M_3-receptor*). Data are representative of three independent experiments. *B,* submandibular glands from wild-type and M_3-muscarinic receptor knock-out mice were fixed in 10% formalin and processed for immunocytochemistry. Sections were stained with antibodies against the total M_3-muscarinic receptor population (*anti-M_3-receptor*) or receptors phosphorylated on serines 384, 412, and 577. Also shown are the DAPI-stained nuclei and the merge of the receptor staining and DAPI. *C,* results shown in *A* and *B* are represented as a bar code describing the relative intensities of receptor phosphorylation on serines 384, 412, and 577 in the different tissues.

efficacy: methacholine = arecoline > pilocarpine (Fig. 8*A*). A similar decrease in the phosphorylation status of spot 2 in Fig. 7 was observed suggesting that spot 2 corresponds to the phosphorylation site Ser^{384}.

Ser^{412} phosphorylation was relatively low in the basal state and was increased equivalently by all three agonists (Fig. 8*B*). This is the same as the effects of the three agonists on the phosphorylation status of spot 4 in Fig. 7, suggesting that spot 4 corresponds to Ser^{412}.

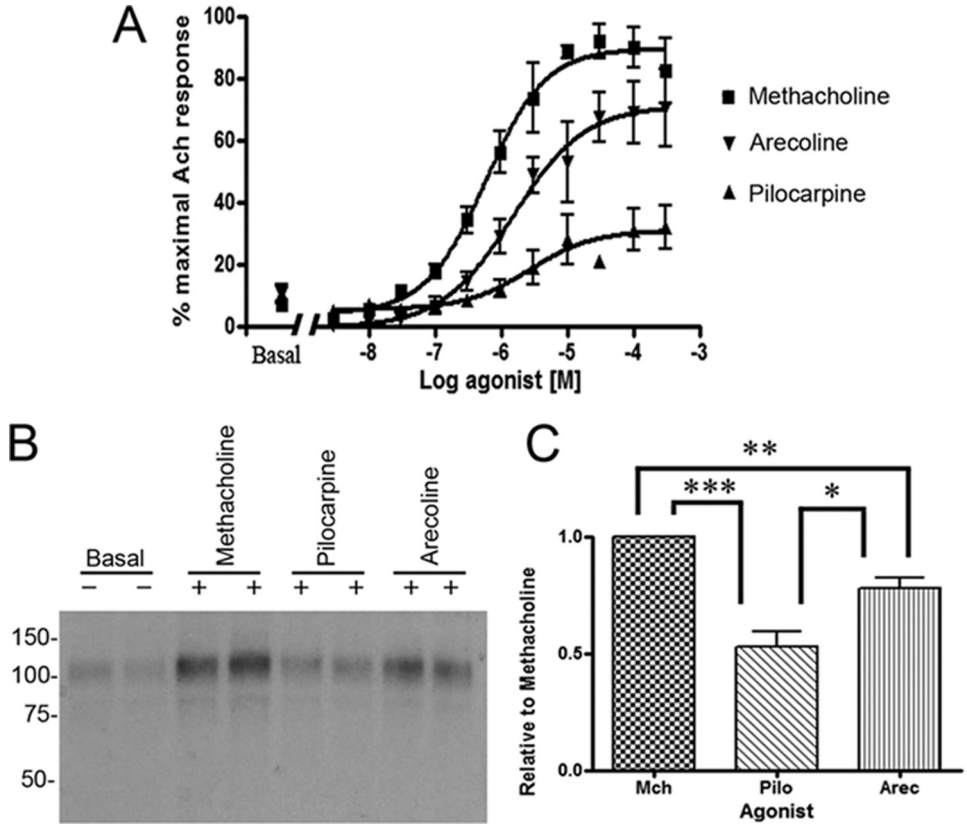

FIGURE 6. **Methacholine-, arecoline-, and pilocarpine-mediated inositol phosphate and receptor phosphorylation response.** *A,* concentration-response curve for methacholine (*Mch*), arecoline (*Arec*), and pilocarpine (*Pilo*) in the inositol phosphate response in CHO-m3 cells. *B,* phosphorylation of the M_3-muscarinic receptor in CHO-m3 cells labeled with [^{32}P]orthophosphate in response to muscarinic receptor agonists. *C,* quantification of the phosphorylation data presented in *B*. *Graphs* represent the means ± S.E. of three independent experiments. *, $p < 0.05$; **, $p < 0.01$; ***, $p < 0.001$ (*t* test).

Finally, phosphorylation of Ser^{577} was increased by all three agonists. The rank order of efficacy was methacholine > arecoline > pilocarpine.

Thus, analysis of the phosphorylation status of the M_3-muscarinic receptor with phospho-specific antibodies indicated that of the phosphorylation sites investigated only agonist-mediated phosphorylation at Ser^{577} followed the expected rank order of efficacy (*i.e.* methacholine > arecoline > pilocarpine). The rank order of efficacy for the changes in phosphorylation at the other two sites (Ser^{384} and Ser^{412}) did not conform to the expected order indicating that agonists were able to direct phosphorylation preferentially at these sites.

DISCUSSION

Studies from our laboratory and from others have raised the possibility that one mechanism by which GPCRs could mediate cell/tissue-specific signaling may be through tissue-specific receptor phosphorylation (4, 5, 12). To test this notion, we addressed here whether a GPCR was phosphorylated in a cell- and tissue-specific fashion. We show that the M_3-muscarinic receptor was indeed differentially phosphorylated in CHO-m3 cells, CG neurons, and MIN6 insulinoma cells. The capacity of this receptor subtype to be differentially phosphorylated was also confirmed by *in vivo* studies where the M_3-muscarinic receptor was found to have a unique phosphorylation profile in the hippocampus, cortex, pancreas, and salivary glands. Thus, this study demonstrates that a GPCR can be phosphorylated in a cell- and tissue-specific manner consistent with the hypothesis that differential phosphorylation could contribute to tissue-specific receptor signaling.

Our study also highlights the complexity of GPCR phosphorylation with the identification of 15 phospho-acceptor sites on the M_3-muscarinic receptor. In addition, we demonstrate the hitherto unobserved phenomenon of agonist-regulated receptor de-phosphorylation. Whereas receptors are known to be de-phosphorylated on withdrawal of the agonist in a process that reactivates internalized receptors (2), the notion that receptors might be phosphorylated in the basal state and then dephosphorylated on agonist stimulation has up to now not been considered. We show here that phosphorylation on Ser^{384} in CHO-m3 cells was decreased following agonist addition. Similarly, we show that a spot identified as spot 2 in the phosphopeptide map in CHO-m3 cells was decreased following methacholine stimulation. We are currently testing if spot 2 in the phosphopeptide map represents the same phospho-acceptor site as Ser^{384}. Importantly, this dephosphorylation event is cell type-specific being restricted to receptors expressed in CHO-m3 cells. In neurons, Ser^{384} phosphorylation was seen to increase on agonist stimulation, and in MIN6 cells basal phosphorylation of Ser^{384} remains unchanged following agonist stimulation. Hence, the example of Ser^{384} reveals the true complexity and flexibility of GPCR

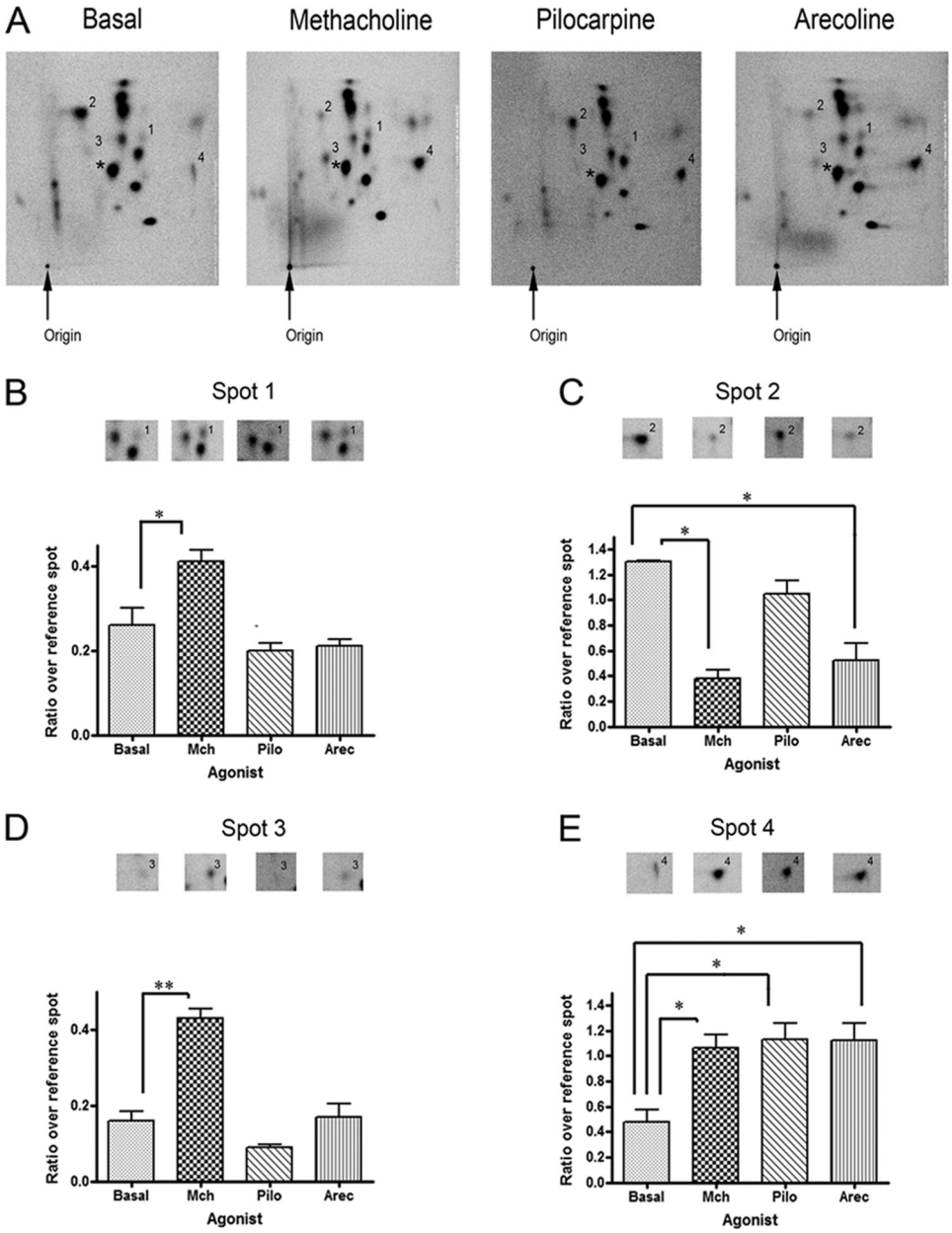

FIGURE 7. **Muscarinic ligands drive preferential receptor phosphorylation.** *A,* tryptic phosphopeptide maps of the M_3-muscarinic receptor expressed in CHO-m3 cells stimulated with a saturating concentration (100 μM) of methacholine (*Mch*), arecoline (*Arec*), or pilocarpine (*Pilo*). Labeled are four spots (*1–4*), which were compared in intensity with the reference spot marked with an *asterisk*. *B–E,* quantification of spots labeled *1–4* in relation to the reference spot. Shown are typical autoradiographs and the cumulative mean data ± S.E. ($n = 3$). *, $p < 0.05$; **, $p < 0.01$ (*t* test).

phosphorylation where a site can remain unchanged or can increase or decrease in its phosphorylation status following agonist stimulation depending on the cell type in which the receptor is expressed.

Are the different patterns of receptor phosphorylation identified here likely to lead to different receptor signaling outcomes? Whereas this is difficult to test *in vivo,* this has been extensively examined in *in vitro* systems. Hence, studies on the β_2-adrenergic receptor have determined that the kinetics of the recruitment of arrestin to the receptor was shown to be dependent on which of the GRKs was employed in receptor phosphorylation (7). That this may impact on signaling was indicated in studies on the CCR7 chemokine receptor where GRK6-mediated phosphorylation leads to ERK1/2 activation, but GRK3 and GRK6 had to be employed in concert to drive receptor internalization and desensitization (12). That members of the GRK family can actually phosphorylate different sites on the same receptor and that these regulate different signaling outcomes have recently been demonstrated for another chemokine receptor CXCR4 (6).

In terms of the M_3-muscarinic receptor, we and others have determined that this receptor subtype is phosphorylated by multiple receptor kinases, including the GRKs, protein kinase CK2, and CK1α (5, 8, 17, 18). It appears that these distinct protein kinases are able to phosphorylate different sites on the receptor and that this results in different functional outcomes (5). Hence, phosphorylation mediated by protein kinase CK2 does not appear to regulate receptor internaliza-

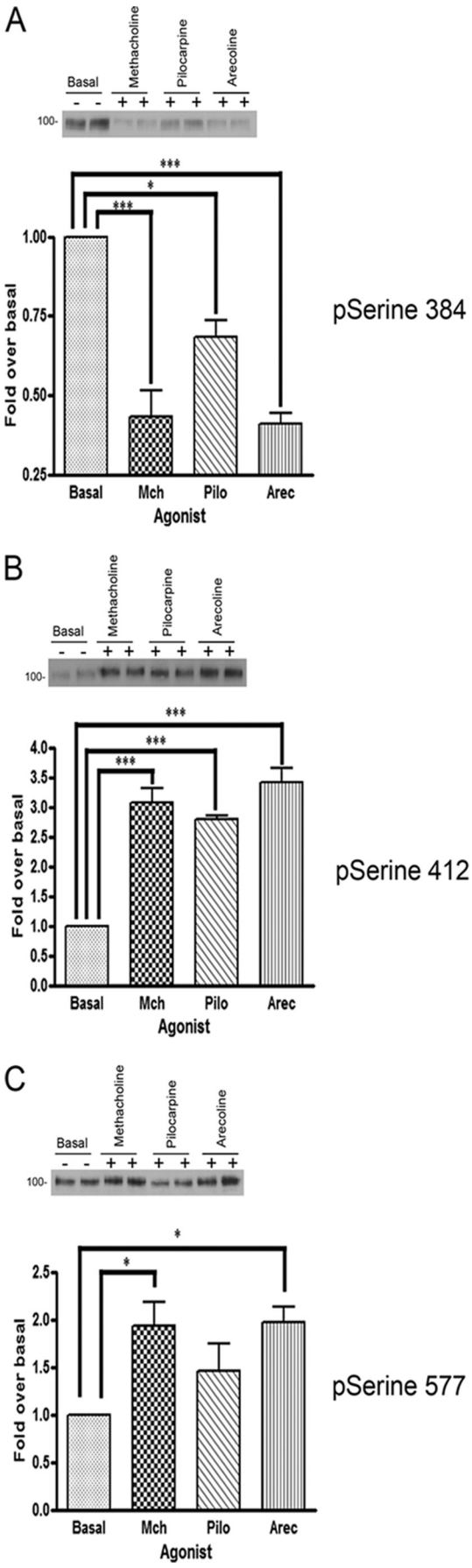

tion nor ERK1/2 activity but rather it regulates the coupling of the receptor to the JUN kinase pathway (5). In contrast, coupling to the ERK1/2 pathway and phosphoinositide signaling is regulated by CK1α-mediated receptor phosphorylation (8, 9), and receptor desensitization and internalization are regulated by the GRKs (17, 19). Thus, these findings on the M_3-muscarinic receptor, coupled to those from other GPCRs, provide compelling evidence that the signaling outcome of GPCRs can be determined by the sites on the receptor that are phosphorylated.

This realization has led to the notion that the pattern of phosphorylation of a receptor can be likened to a bar code that encodes a particular signaling outcome that could be employed in a tissue-specific manner to fine-tune the signaling outcome of a receptor to match a particular physiological role (3, 10–12). Such a concept was first proposed to account for the different signaling outcomes mediated by various members of the GRK family on the angiotensin II receptor and V2 vasopressin receptor (10, 11). If this notion were correct, then GPCRs would be expected to show cell/tissue-specific phosphorylation. Hence, the data presented here describing different phosphorylation profiles of a GPCR in different cell/tissue types support the notion of a phosphorylation bar code (Fig. 5*C*) being employed to drive tissue-specific receptor signaling.

It is therefore likely that at any given point a single receptor molecule will display a specific pattern of phosphorylation that is binary in a manner analogous to a bar code. It should be noted, however, that not all of the receptors in a tissue will necessary have the same phosphorylation bar code. Thus, a population of receptors will reflect the average phosphorylation profile and as such will show different intensities at specific sites.

The phosphorylation bar code adopted by a receptor will be a reflection of the receptor conformation following agonist occupation (see below) but also the complement of protein kinases and phosphatases employed. We know that the M_3-muscarinic receptor can be phosphorylated by a range of protein kinases, including GRK2, GRK6, CK1α, and protein kinase CK2 (5, 8, 17, 18). It is possible that these kinases are employed differentially to mediate tissue-specific phosphorylation (3).

We extended our studies further by asking if different ligands could mediate different patterns of phosphorylation. This study was conducted in the knowledge that there is a growing list of receptor ligands that are able to direct signaling of receptors preferentially to one signaling pathway over another (20). This phenomenon has been variously described as ligand-directed trafficking, ligand bias, and functional selectivity (21–23). The importance of this for the physiological

FIGURE 8. **Phospho-specific antibodies reveal the capacity of ligands to drive preferential M_3-muscarinic receptor phosphorylation.** CHO-m_3 cells were stimulated with a saturating concentration (100 μM) of methacholine (*Mch*), arecoline (*Arec*), or pilocarpine (*Pilo*). The cells were then lysed, and the receptor was immunoprecipitated with a receptor monoclonal antibody. The immunoprecipitate was then probed with receptor phospho-specific antibodies against phosphoserine 384 (*A*), phosphoserine 412 (*B*), and phosphoserine 577 (*C*). Shown are typical autoradiographs and the cumulative mean data ± S.E. ($n = 3$). *, $p < 0.05$; ***, $p < 0.001$ (*t* test).

role of the M_3-muscarinic receptor has recently been highlighted in studies from our laboratory that have determined that the mechanism by which this receptor subtype regulates hippocampus-based memory and learning is via signaling through a receptor phosphorylation/arrestin-dependent pathway in preference to signaling via heterotrimeric G-proteins (13).

We show here that the efficacy of three muscarinic ligands, methacholine (full agonist), arecoline (partial agonist), and pilocarpine (partial agonist), in mediating overall receptor phosphorylation correlated with the efficacy of these ligands in the activation of inositol phosphate signaling. Similar correlations have been made for agonists at the β_2-adrenergic receptor where phosphorylation was measured in relation to the maximal response of a series of full and partial agonists (24). In this study, this correlation was not, however, maintained if individual sites of phosphorylation were measured either in phosphopeptide maps or by use of phospho-specific antibodies. Hence, agonist-mediated phosphorylation of spot 4 in the phosphopeptide map in Fig. 7 and phosphorylation at Ser^{412} (Fig. 8) showed that all three agonists were full agonists in stimulating an increase in phosphorylation at these sites.

Hence, the break from the expected rank order of efficacy observed for Ser^{412} and spot 4 indicates that the impact that the ligands have on phosphorylation is not equivalent for all sites. That this is the case is further supported by studies on the CXCR4 and somatostatin receptor where agonists have been identified that are able to regulate receptor phosphorylation differently (6). Thus, the data from this study raise the possibility that ligands can preferentially direct receptor phosphorylation. This being the case, it would seem plausible that ligands that show a bias toward arrestin/phosphorylation signaling may do so because they have the quality of driving preferential phosphorylation of receptors in a manner that promotes signaling through this pathway in preference to signaling through other pathways.

In conclusion, our study supports the hypothesis that one mechanism that is employed by biased ligands to direct receptor signaling is the capacity of ligands to preferentially drive receptor phosphorylation. Furthermore, the data presented here also highlight the fact that GPCRs can be phosphorylated in a cell and tissue type-specific fashion in a manner that would provide a mechanism for cell/tissue-specific receptor signaling.

Acknowledgments—We thank Dr. Jurgen Wess (National Institutes of Health, Bethesda) for providing the M_3-muscarinic receptor knock-out mice.

REFERENCES

1. Reiter, E., and Lefkowitz, R. J. (2006) *Trends Endocrinol. Metab.* **17,** 159–165
2. Premont, R. T., and Gainetdinov, R. R. (2007) *Annu. Rev. Physiol.* **69,** 511–534
3. Tobin, A. B., Butcher, A. J., and Kong, K. C. (2008) *Trends Pharmacol. Sci.* **29,** 413–420
4. Tobin, A. B. (2008) *Br. J. Pharmacol.* **153,** S167–S176
5. Torrecilla, I., Spragg, E. J., Poulin, B., McWilliams, P. J., Mistry, S. C., Blaukat, A., and Tobin, A. B. (2007) *J. Cell Biol.* **177,** 127–137
6. Busillo, J. M., Armando, S., Sengupta, R., Meucci, O., Bouvier, M., and Benovic, J. L. (2010) *J. Biol. Chem.* **285,** 7805–7817
7. Violin, J. D., Ren, X. R., and Lefkowitz, R. J. (2006) *J. Biol. Chem.* **281,** 20577–20588
8. Luo, J., Busillo, J. M., and Benovic, J. L. (2008) *Mol. Pharmacol.* **74,** 338–347
9. Budd, D. C., Willars, G. B., McDonald, J. E., and Tobin, A. B. (2001) *J. Biol. Chem.* **276,** 4581–4587
10. Kim, J., Ahn, S., Ren, X. R., Whalen, E. J., Reiter, E., Wei, H., and Lefkowitz, R. J. (2005) *Proc. Natl. Acad. Sci. U.S.A.* **102,** 1442–1447
11. Ren, X. R., Reiter, E., Ahn, S., Kim, J., Chen, W., and Lefkowitz, R. J. (2005) *Proc. Natl. Acad. Sci. U.S.A.* **102,** 1448–1453
12. Zidar, D. A., Violin, J. D., Whalen, E. J., and Lefkowitz, R. J. (2009) *Proc. Natl. Acad. Sci. U.S.A.* **106,** 9649–9654
13. Poulin, B., Butcher, A., McWilliams, P., Bourgognon, J. M., Pawlak, R., Kong, K. C., Bottrill, A., Mistry, S., Wess, J., Rosethorne, E. M., Charlton, S. J., and Tobin, A. B. (2010) *Proc. Natl. Acad. Sci. U.S.A.* **107,** 9440–9445
14. Tobin, A. B., and Nahorski, S. R. (1993) *J. Biol. Chem.* **268,** 9817–9823
15. Lee, H. M., Tsai, K. J., Lin, C. H., Huang, C. L., and Tung, C. S. (1998) *J. Neurochem.* **70,** 1189–1198
16. Szekeres, P. G., Koenig, J. A., and Edwardson, J. M. (1998) *Mol. Pharmacol.* **53,** 759–765
17. Willets, J. M., Challiss, R. A., Kelly, E., and Nahorski, S. R. (2001) *Mol. Pharmacol.* **60,** 321–330
18. Tobin, A. B., Totty, N. F., Sterlin, A. E., and Nahorski, S. R. (1997) *J. Biol. Chem.* **272,** 20844–20849
19. Tsuga, H., Okuno, E., Kameyama, K., and Haga, T. (1998) *J. Pharmacol. Exp. Ther.* **284,** 1218–1226
20. Violin, J. D., and Lefkowitz, R. J. (2007) *Trends Pharmacol. Sci.* **28,** 416–422
21. Drake, M. T., Violin, J. D., Whalen, E. J., Wisler, J. W., Shenoy, S. K., and Lefkowitz, R. J. (2008) *J. Biol. Chem.* **283,** 5669–5676
22. Kenakin, T. (2007) *Trends Pharmacol. Sci.* **28,** 407–415
23. Urban, J. D., Clarke, W. P., von Zastrow, M., Nichols, D. E., Kobilka, B., Weinstein, H., Javitch, J. A., Roth, B. L., Christopoulos, A., Sexton, P. M., Miller, K. J., Spedding, M., and Mailman, R. B. (2007) *J. Pharmacol. Exp. Ther.* **320,** 1–13
24. Tran, T. M., Friedman, J., Qunaibi, E., Baameur, F., Moore, R. H., and Clark, R. B. (2004) *Mol. Pharmacol.* **65,** 196–206
25. Yamada, M., Miyakawa, T., Duttaroy, A., Yamanaka, A., Moriguchi, T., Makita, R., Ogawa, M., Chou, C. J., Xia, B., Crawley, J. N., Felder, C. C., Deng, C. X., and Wess, J. (2001) *Nature* **410,** 207–212